THE BELL SYSTEM TECHNICAL JOURNAL
Vol. 59, No. 8, October 1980
Printed in U.S.A.

High-Speed Digital Lightwave Communication Using LEDs and PIN Photodiodes at 1.3 μm

By D. GLOGE, A. ALBANESE, C. A. BURRUS, E. L. CHINNOCK, J. A. COPELAND, A. G. DENTAI, T. P. LEE, TINGYE LI, and K. OGAWA

(Manuscript received April 9, 1980)

At the wavelength of 1.3 μm, fiber loss and dispersion are sufficiently small that many lightwave communications applications can use simple and reliable LED transmitters and PIN photodiode receivers without avalanche gain. Bit rates can be as high as several hundred Mb/s. With new high-speed devices based on III–V semiconductors and microwave silicon IC technology, we have designed two fully retimed optical regenerators that operate at 1.3 μm and at bit rates of 44.7 and 274 Mb/s to study the potential of the LED-PIN approach. A detailed analysis of the baseband characteristics of the LED, the fiber, and the receiver leads to an overall equalization approach that minimizes receiver noise. The success of this performance optimization is corroborated by bit-error measurements under simulated system conditions. The results suggest repeaterless operation over distances up to 24 km at 44.7 Mb/s and 8 km at 274 Mb/s for a cable loss of 1 dB/km and a bandwidth of 1000 MHz·km. The use of lasers in such multimode fiber sytems would permit larger margin allocations and penalties than those chosen for LED systems, but would not lead to substantially longer repeater spacings.

I. INTRODUCTION

Optical-fiber communication systems that use LEDs as sources and PIN photodiodes as detectors offer the attractive features of reliability, simplicity, and low cost. Operation of such systems at high digital speeds is now made possible by the availability of InGaAsP LEDs and detectors, and of low-loss fibers that exhibit minimal material dispersion in the wavelength region near 1.3 μm.[1] The bandwidth-distance product at the wavelength of minimum dispersion is inversely proportional to the square of the spectral width of the source and, for germania-doped silica fibers, is 3.5 GHz·km or more if surface-emitting

LEDs are used.[2] Thus high-speed digital systems of a few hundred Mb/s can be operated over repeater spans of 5 to 10 km.

An earlier paper[3] presented a discussion of material-dispersion-limited operation of fiber systems that use LEDs and reported an experiment that showed the effects of material dispersion on a 137-Mb/s data link operating at $\lambda = 0.89$ or 1.20 μm. In the present paper, we discuss further the application of LEDs and PIN photodiodes in high-speed digital fiber systems and describe two optical repeater experiments (with bit rates of 44.7 and 274 Mb/s) at $\lambda = 1.3$ μm using InGaAsP LEDs as transmitters and InGaAs PIN photodiodes followed by GaAsFET preamplifiers as receivers. Experimental results are compared with theory.

II. SYSTEM CONSIDERATIONS

For high-speed digital applications, the characteristics of the LED that are important are its reliability, output power, modulation bandwidth, spectral width, and temperature behavior. The reliability of high-radiance, surface-emitting InGaAsP LEDs is now well established, as results from accelerated-aging tests at elevated temperatures project a mean life in excess of 5×10^9 hours for room-temperature operation.[4] Sufficient power at $\lambda = 1.3$ μm is available from these devices: peak powers of 200 μW have been coupled into large-core step-index optical fibers.[4,5] The modulation bandwidth of an LED depends on the device geometry, the current density, and the doping concentration and width of the active region; a high doping concentration or a narrow active region results in large bandwidth but yields low output power.[6]

The fall-off of the modulated output power $P_s(f)$ of an LED as a function of the modulating frequency f can be described by the function

$$H_s(f) = (1 + if/b)^{-1}, \tag{1}$$

where b is the modulation bandwidth of the LED defined at the half-power point (3-dB electrical). For high-radiance surface-emitting diodes, typical values of the average power $\bar{P}_s$ that can be coupled into standard multimode fibers (50-μm core diameter, 0.23 N.A.) are $\bar{P}_s \simeq 50$ μW for $b = 50$ MHz. In general, $\bar{P}_s$ is proportional to $b^{-\nu}$ where $\nu \leq 1$. For moderately fast, double-heterostructure GaAlAs surface emitters, $\nu = \frac{2}{3}$ is a typical value.[6] LEDs with bandwidths in excess of 1 GHz have been fabricated;[7] the output of these very fast diodes tends to decrease as $1/b$.

Compared to an injection laser, the output power of the LED is rather insensitive to temperature variations. Observed data on the performance of the LED used in our repeater experiments are given in Section III.

Microwave GaAsFETs are ideally suited for use as low-noise pream-

plifiers following the PIN photodetector in an optical receiver because they have low input gate capacitances and high-transconductances.[8,9] The sensitivity of an optical receiver using state-of-the-art PIN photodiodes and GaAsFETs can be made to fall within a few decibels of that of the typical silicon avalanche photodiode receiver used presently in fiber systems that operate at $\lambda = 0.85\ \mu m$.[10,11] At longer wavelengths, significant bulk leakage currents at voltages approaching breakdown severely limit the use of avalanche gain as a low-noise amplification process. For this reason, very low-noise preamplifiers will play a key role in future long-wavelength systems.

We make use of Personick's theory[12] to calculate the receiver sensitivity, which can be expressed in terms of N_r, the average number of signal photoelectrons per bit required at the detector to yield an error probability of 10^{-9}. N_r is given by three terms which account for Johnson, shot and FET channel noise:

$$N_r = \frac{6}{qB}\left\{\frac{4kT}{R_L}J_2B + 2qI_LJ_2B + 16\pi^2kT\Gamma\left[\frac{C_T^2}{g_m}\right]J_3B^3\right\}^{1/2}, \quad (2)$$

where

q = electronic charge
B = bit rate
k = Boltzmann's constant
R_L = equivalent input resistance
I_L = total leakage current (photodiode and FET)
Γ = noise factor associated with channel noise in the FET and is taken to be 1.15 for a GaAsFET with negligible gate noise[12,13]
T = absolute temperature in degrees Kelvin
C_T = total capacitance (photodiode, FET and stray)
g_m = transconductance of the FET.

The coefficients J_2 and J_3 account for the noise distribution in the receiver channel and are discussed subsequently.

Figure 1 presents receiver sensitivity estimates using eq. (2), assuming R_L to be infinite and the best available devices to have $g_m = 30$ mS and $C_T = 1.5$ pF. For $I_L = 0$, N_r is proportional to $C_T/\sqrt{g_m}$. The dashed diagonal lines help to determine the sensitivity in terms of the average optical power

$$\bar{P}_r = N_r hcB/\lambda\eta \quad (3)$$

required at the receiver, where h is Planck's constant and c is the speed of light. They are computed for a wavelength $\lambda = 1.3\ \mu m$ and an external quantum efficiency $\eta = 0.7$.

Figure 1 also indicates the performance degradation resulting from leakage or dark current in the FET and the photodiode. Such currents

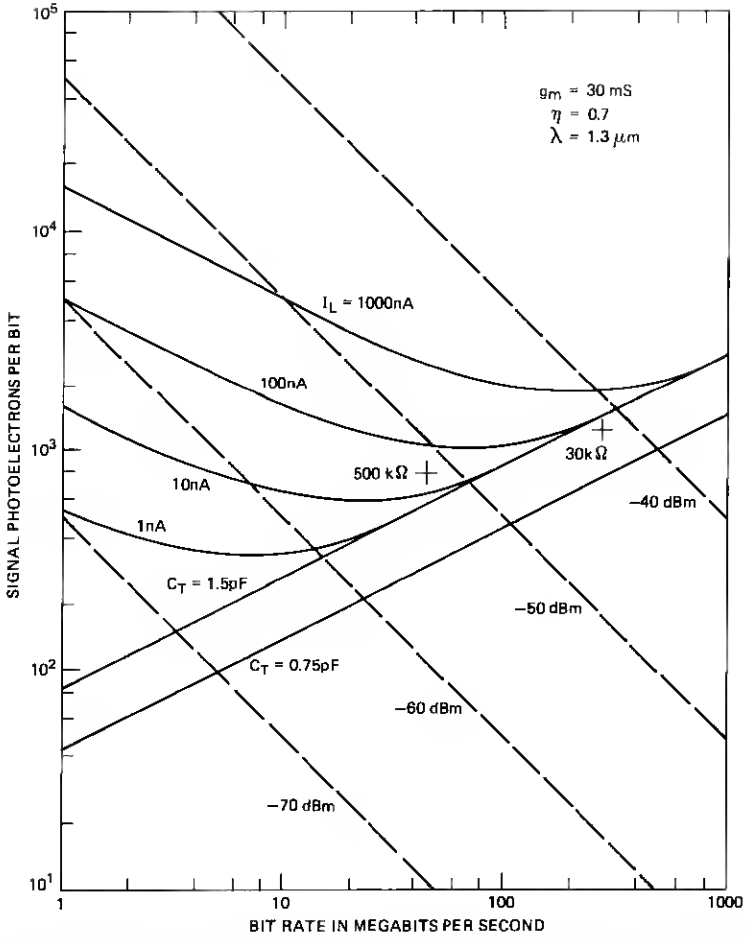

Fig. 1—Average number of photoelectrons per bit vs bit rate according to eq. (2) required for error probability of 10^{-9}; optical receiver uses PIN-GaAsFET front-end with total input capacitance C_T, leakage current I_L, and transconductance g_m = 30 mS. Dashed lines indicate average optical power required at the receiver for quantum efficiency $\eta = 0.7$ and wavelength $\lambda = 1.3$ μm.

can be as high as 200 nA at typical elevated operating temperatures (see Sections III and IV). Another noise phenomenon, $1/f$ noise, is not indicated in Fig. 1, but is discussed briefly at the end of Section IV. A similar performance evaluation on the basis of Personick's theory has been conducted for receivers using the most advanced silicon bipolar transistors (C_T = 2pF, current gain β = 300). The results are listed in Table I for some bit rates of interest. Also listed is the expected performance for the case of an avalanche photodiode followed by a GaAs FET amplifier. In this case, we assume a maximum bulk leakage

Table I—Comparison of expected sensitivity of three types of receivers

Bit Rate	44.7 Mb/s	274 Mb/s	1096 Mb/s
PIN/(Si)Bipolar	−45 dBm	−38 dBm	−32 dBm
PIN/(GaAs)FET	−50 dBm	−40 dBm	−32 dBm
APD/(GaAs)FET		−43 dBm	−38 dBm

current of 200 nA before multiplication and a carrier-ionization ratio of 4:1.

The use of J_2 and J_3 in eq. (2) is based on the assumption that the digital information arrives undistorted at the receiver input and is transformed by the receiver filter function $H_r(f)$ for minimum noise and intersymbol interference. In this case,

$$J_{n+2} = \frac{1}{B}\int_0^B \left|\frac{f}{B}\right|^{2n} \left|H_r\right|^2 df. \tag{4}$$

Table II lists J_n for a non-return-to-zero signal format and a raised-cosine signal spectrum at the receiver output, in which case $H_r = (\pi f/2B)\cot(\pi f/2B)$.

In general, the signal arriving at the receiver has been modified by the response of tbe source, $H_s(f)$, and the response of the transmission medium, $H_t(f)$. To compensate for these effects, the receiver must be designed with a response $H_r' = H_r/H_sH_t$. As a first example, consider the case of an LED with response given by eq. (1) and unlimited fiber bandwidth. Let FET channel noise be the dominant noise contribution as described by the third term in eq. (2). The coefficient J_3 in that term now becomes $J_3 + J_4\,(B/b)^2$ because H_r in eq. (4) is replaced by H_r'. Hence the required receiver power becomes $\bar{P}_r' = \bar{P}_r[1 + (J_4/J_3)(B/b)^2]^{1/2}$ where $\bar{P}_r$ is the value previously computed from eqs. (2) and (3). This degradation of receiver sensitivity represents the power penalty one pays for equalizing the response of the LED.

The available optical signal margin between transmitter and receiver is proportional to $\bar{P}_s/\bar{P}_r'$, where $\bar{P}_s$ is the average power at the transmitter as defined earlier. For $\bar{P}_s$ proportional to $b^{-\nu}$, the function $\bar{P}_s/\bar{P}_r'$ has a maximum at $b = B\left(\frac{1}{\nu} - 1\right)^{1/2}(J_4/J_3)^{1/2}$ or $b = 0.42B$ if ν

Table II—Values of J_n

J_2	0.5628
J_3	0.0868
J_4	0.0304
J_5	0.0143
J_6	0.0079
J_7	0.0048

= ⅔. The latter condition results in a degradation of receiver sensitivity (or an equalization penalty) of 2.4 dB over the values given in Fig. 1. A faster LED would reduce this penalty, but would provide less output power and a smaller overall signal margin.

Chromatic and intermodal dispersion in the fiber also influence the signal. Neglecting nonlinear, coherence and waveguide effects, we can model the fiber transfer characteristic by the product of two filter functions H_c and H_d, one describing material dispersion and the other, intermodal delay differences. For a given transmission distance z, the material effect can be determined in advance for typical LED systems and can be compensated for in the receiver filter. At the wavelength of minimum material dispersion (~1.3 μm), the transfer function attributable to material dispersion is[2]

$$H_c(f) = (1 + i\pi f z\sigma^2/10c\lambda^2)^{-1/2} \tag{5}$$

for a Gaussian LED spectrum having an rms width $\sigma = 0.425$ FWHM. For typical InGaAsP LEDs with a doping density of 3×10^{18} cm^{-3}, the rms width is $\sigma = \lambda^2/40$ μm, where λ is in μm.[14]

Figure 2 shows the increase in the required receiver power as a result of material dispersion in fibers plotted against the product of bit rate B and transmission distance z. The LED bandwidth b is used as a parameter. The penalties associated with transfer functions given by eqs (1) and (5) add nearly linearly.

Present fiber fabrication processes are not sufficiently precise to provide the desired control of intermodal delays (less than ~0.5 ns/km total). Thus, unable to anticipate the resulting baseband characteristics precisely, we must also allow for an equalization penalty due to intersymbol interference in addition to that caused by first-order equalization in the receiver. To estimate the latter effect, we use the simple functional dependence

$$H_d(f) = (1 + i\sqrt{3}\, zf/Q)^{-1} \tag{6}$$

following the usual notation of a bandwidth-distance product Q defined at $|H_d| = ½$ (3 dB optical). The additional penalty factor $[1 + 3(J_4/J_3)(zB/Q)^2]^{1/2}$ can be calculated in a manner similar to that described above for the source.

III. EXPERIMENTAL LEDs AND PIN PHOTODIODES

The high-radiance light-emitting-diode structure used in this work is shown in Fig. 3. The diode was a small-area, etched-well surface emitter, described previously,[15] made from a double-heterostructure wafer of InP/$In_{1-x}Ga_xAs_yP_{1-y}$/InP grown by liquid-phase epitaxy. The composition of the quaternary active layer ($x = 0.36$, $y = 0.80$) was chosen to produce diodes with an output wavelength of 1.3 μm ± 0.05

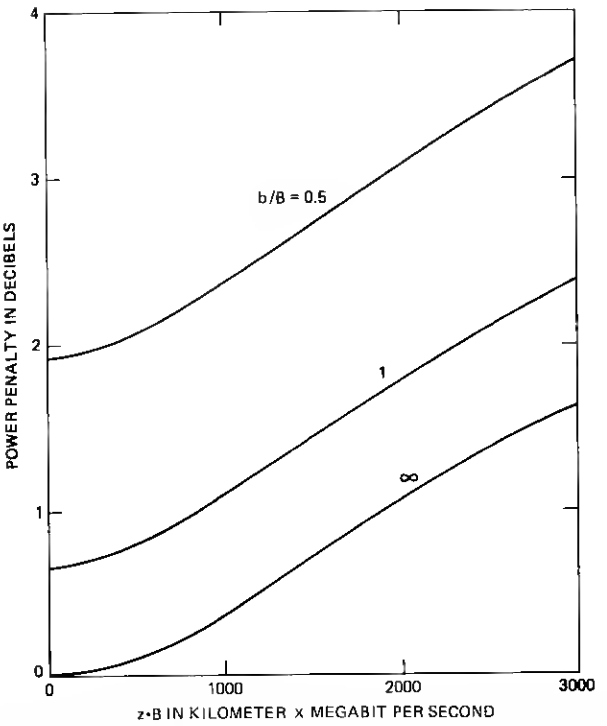

Fig. 2—Increase in optical signal power required at the receiver as a result of material dispersion in germanosilicate multimode fibers plotted vs product of distance z and bit rate B; b is the LED modulation bandwidth.

μm, under room-temperature ambient conditions, at an operating current of 100 mA dc. This current corresponds to a current density of about 5 kA/cm^2 in the primary emitting area, which was about 50 μm in diameter. The active quaternary layer, 1 to 1.5 μm thick, was doped p-type with zinc to a relatively high carrier concentration of 2 to 4 $\times$ 10^{18}/cm^3. The 1.3-μm wavelength output into the air without antireflection coatings or lenses was about 1 mW at 100 mA. A typical multimode fiber (50-μm core diameter, 0.23 N.A.), butt-coupled without index matching, collected 10 μW of that power. The spectral width (FWHM) at 25°C and 100 mA was 1145Å. The electrical modulation bandwidth was ≈170 MHz.

Temperature characteristics of the diodes were measured in the range of 20°C to 100°C, and the output power was found to follow approximately the relation

$$P_T = P_o \exp[-(T - T_o)/T_c], \tag{7}$$

where P_o is the power output at T_o (300°K) and the characteristic temperature, T_c, is 80°K. These results are plotted in Fig. 4, where it

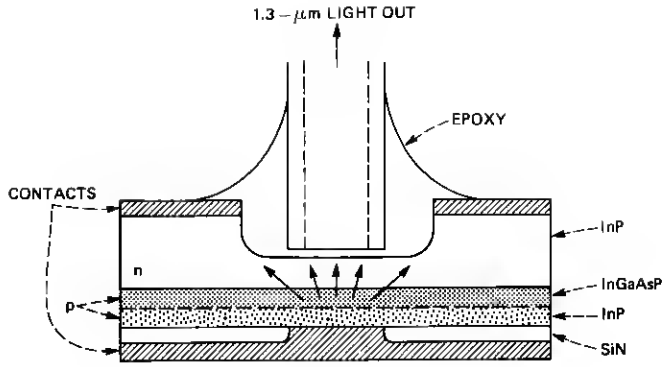

Fig. 3—Schematic cross section of the 1.3-μm LED.

can be seen that the output was reduced by 1.5 dB for a temperature rise from room temperature to 55°C. The thermal impedance was 80 to 100°C/W. The peak emission wavelength was shifted 380Å at a rate of ~5Å/°C toward longer wavelengths by the same temperature increase. The spectral width varied approximately as λ^2. The electrical

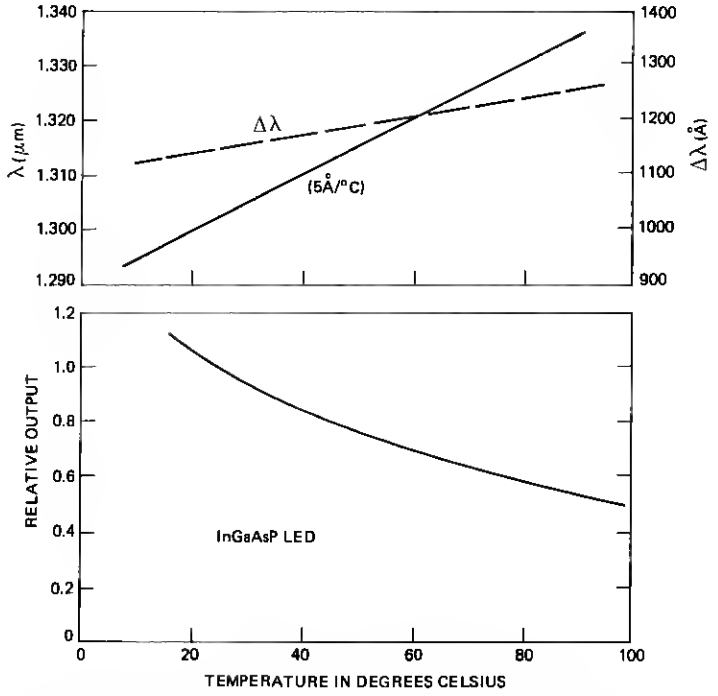

Fig. 4—Temperature dependence of wavelength, spectral width (FWHM) and output of the 1.3-μm InGaAsP LED.

modulation bandwidth, however, remained unchanged from 20 to 100°C. The practical operating life of these specific diodes is unknown, but at this writing, similar unencapsulated diodes have been operating at 100 mA dc in a room-temperature laboratory environment for over 23,000 hours with negligible degradation.

Photodetectors for the experiment were PIN photodiodes made with $In_xGa_{1-x}As$ lattice matched to InP ($x = 0.53$). They are described in more detail elsewhere.[16] This ternary composition has a bandgap energy of 0.75 eV, corresponding to a long-wavelength cutoff near 1.65 μm. The attainable leakage current of p-n junctions in this material has proved to be one to two orders of magnitude less (better) than that associated with similar junctions in germanium, but otherwise the photosensitive properties of the two materials are rather similar.

The InGaAs was grown by a conventional LPE technique to a thickness of 6 to 8 μm on a ⟨100⟩ n-type InP substrate. The epitaxial layer was not intentionally doped and, with a suitable bake-out[17] of the boat and starting materials before growth, the residual n-type carrier concentration of the ternary layer was 1 to $2 \times 10^{15}/cm^3$. This relatively low impurity concentration permits the fabrication of diodes with low capacitance and depletion layer widths of 2 to 3 μm at low bias voltages.[16,17]

The photodiodes are illustrated schematically in Fig. 5. The p-n junction was prepared by diffusion of zinc to a depth of 2.5 to 3.5 μm into the grown InGaAs layer. After contacts were applied, small mesas with a diameter of about 90 μm were formed by chemical etching and windows about 250 μm in diameter were opened in the substrate

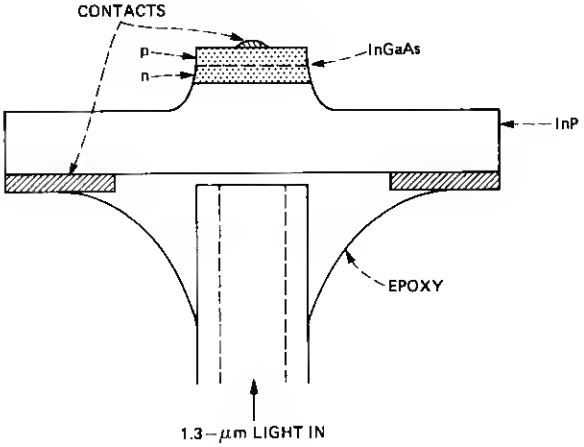

Fig. 5—Schematic cross section of the back-illuminated long-wavelength PIN photodiode.

metallization, also by chemical etching, to permit unobstructed illumination of the junction through the substrate. This back-illuminated configuration takes advantage of the transparency of the InP substrate to minimize absorption loss and surface recombination and, at the same time, to achieve minimum dark current and minimum parasitic capacitance: there is no need to enlarge the junction area to provide room for contacts or contacting pads. The diodes were operated without an anti-reflection coating, and the external quantum efficiency approached the transmission coefficient of 0.7 expected at the interface between air and InP (refractive index 3.4).

The 90-μm mesas had measured junction capacitances of 1 to 1.5 pF at zero bias and 0.3 to 0.5 pF at 10 V reverse bias, where the depletion width was about 3 μm and the peak electric field was estimated to be 6.7×10^4V/cm. The best units had dark currents between 1 and 2 nA at 25°C and 10V reverse bias; the variation of the dark current with temperature was $\exp(-E_g/2kT)$ up to 100°C (see Fig. 6). The dark current of the units used in the present repeater experiment ranged

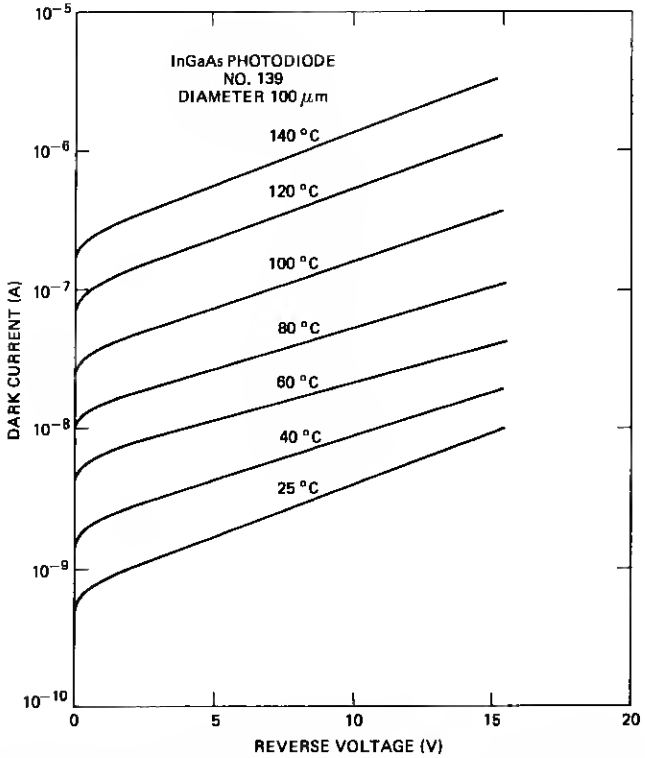

Fig. 6—Dark-current characteristics of one of the best InGaAs diodes in the temperature range between 25 and 100°C.

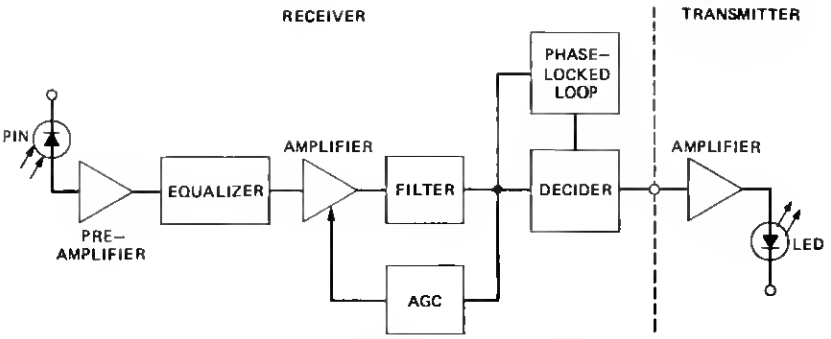

Fig. 7—Block diagram of the optical repeater.

from 5 to 100 nA at room temperature. The reverse breakdown was 75 to 100 V at 10-μA bias current. The parasitic capacitance of the modified silicone-potted "pill" package used in these experiments was 0.1 to 0.15 pF. The measured rise times of the better units were less than 0.2 ns.

IV. REGENERATOR DESIGN

To test the feasibility of the system configuration described earlier, we assembled two experimental regenerators designed to operate at 44.7 and 274 Mb/s. Figure 7 shows a block diagram of the essential functions. The transmitter module was the same for both regenerators and consisted of a two-stage GaAs FET power amplifier driving the LED previously described. The amplifier produced pulses of 200-mA peak current and 500-ps rise time. With this design, it was possible to generate pseudo-random optical pulse patterns at bit rates up to 365 Mb/s. Figure 8 shows the transmitter output at 274 Mb/s. The average power launched into a fiber of 50-μm core diameter and 0.23 N.A. was about 5 μW.

The receiver module consisted of the linear amplifier and filter, decision, and timing recovery circuits. Except for the timing recovery function, the 274-Mb/s design made use of high-speed integrated circuits based on the microwave isolated-junction technology. The timing recovery circuit used was a standard part of the Western Electric regenerator designed for the T4M coaxial transmission system.[18] The linear channel consisted of the optical detector, a GaAs FET preamplifier described below, an equalizer, a 60-dB booster amplifier with automatic gain control, and a multistage LC filter designed to produce the desired noise characteristic.[11] The booster and regenerator portions of the 44.7-Mb/s regenerator were standard parts presently used in the FT3 lightwave transmission system.[19]

The front-end portions of both regenerators consisted of the InGaAs

detector previously described, a low-noise dc-coupled feedback amplifier as shown in Fig. 9 and an RC equalizing circuit. The three-stage amplifier was comprised of a GaAs FET and two complementary microwave transistors.[11] The critical circuit parameter was the input capacitance C_T, which consisted of the photodiode capacitance (0.5 pF), the FET gate-source capacitance (0.5 pF), and the parasitic circuit capacitance (0.5 pF). With $C_T = 1.5$ pF and $g_m = 30$ mS, the performance resulting from FET channel noise can be found in Fig. 1.

The extraordinary speed of the microwave transistors used ($f_c = 4$ GHz), as well as a special computer-aided circuit design process, made it possible to construct a feedback amplifier useful at bit rates up to several hundred megabits per second. This approach assured wide amplifier bandwidth, wide dynamic range, and a single-pole characteristic which minimized the subsequent equalization required. Figure 10 shows the test package with coaxial connections. The open-loop gain A and the feedback resistance R_L were chosen as indicated in Table III. The objective was to maximize the bandwidth of the feedback amplifier, which is roughly proportional to A/R_LC_T, without adding significant front-end noise. The first term in eq. (2) describes the noise

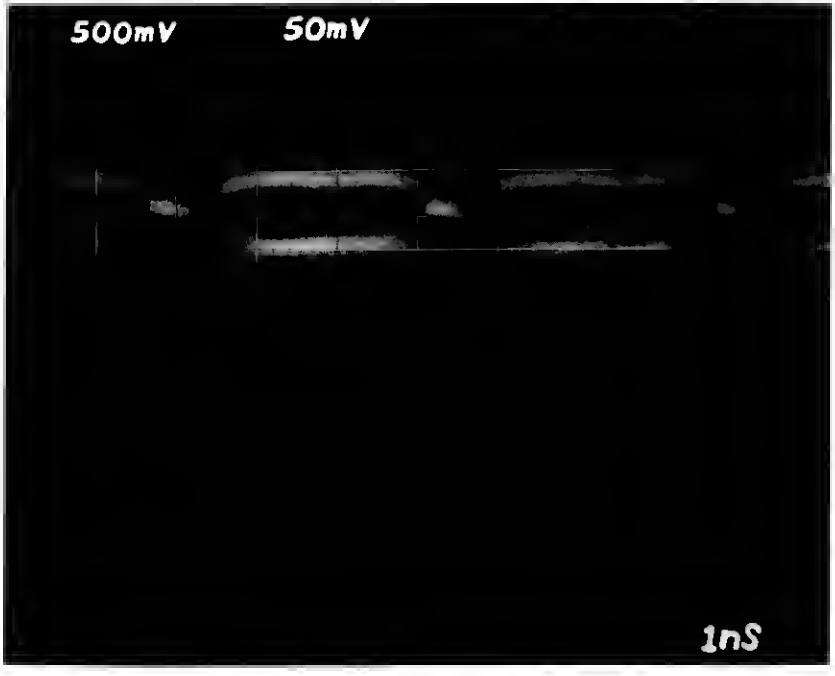

Fig. 8—Eye diagram at the transmitter output ($B = 274$ Mb/s).

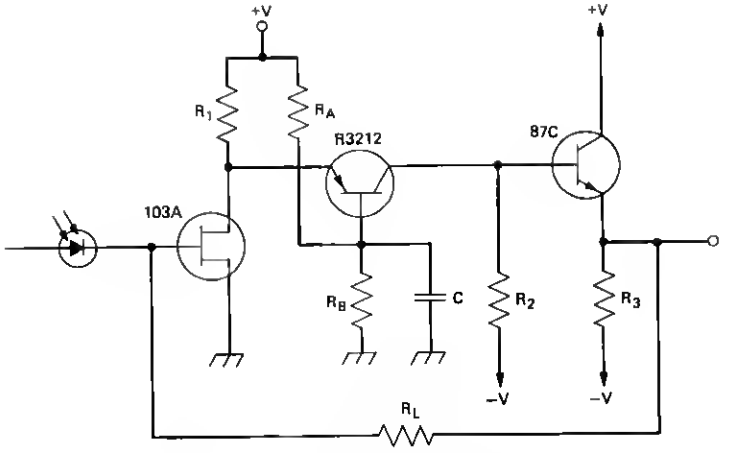

Fig. 9—GaAsFET preamplifier circuit diagram.

contribution due to R_L; for the two cases listed in Table III, the noise contributions are shown in Fig. 1 by the two crosses.

The gate leakage current of the GaAs FETs was a function of temperature and gate bias voltage. For an operating bias V_{GS} of −0.5 V, the best units had a leakage current of 1 to 2 nA which increased to 5 to 10 nA at 70°C.[20] As in the case of the detector diode, there was a significant spread in performance, but most of the results described below were obtained with units not specially selected. At bit rates below 100 Mb/s, the $1/f$ noise component of the GaAs FET can impair the sensitivity of the PIN-FET receiver. We found this degradation to be negligible to bit rates as low as 30 Mb/s in all units employed in our receiver studies.

V. EXPERIMENTAL RESULTS AND CONCLUSIONS

Two system experiments were performed, one at each bit rate, by connecting the transmitter and receiver modules shown in Fig. 7 via multimode test fibers. Pseudo-random bit patterns were transmitted at the design rate and the system was tested for bit errors. Figure 11 shows the results. The solid lines are best fits to the data points.

For comparison with theory, one can compute $\bar{P}_r$ from eqs. (2) and (3) using g_m = 50 mS, C_T = 1.5 pF, R_L from Table III and I_L = 75 nA as measured for the combined leakage current of the FET and the photodiode. The external quantum efficiency of the detector in the 44.7-Mb/s receiver was 0.50, while for the 274-Mb/s receiver η was 0.66. With these values, we calculate an expected receiver sensitivity of −49.7 dBm at 44.7 Mb/s and −39.8 dBm at 274 Mb/s, on the

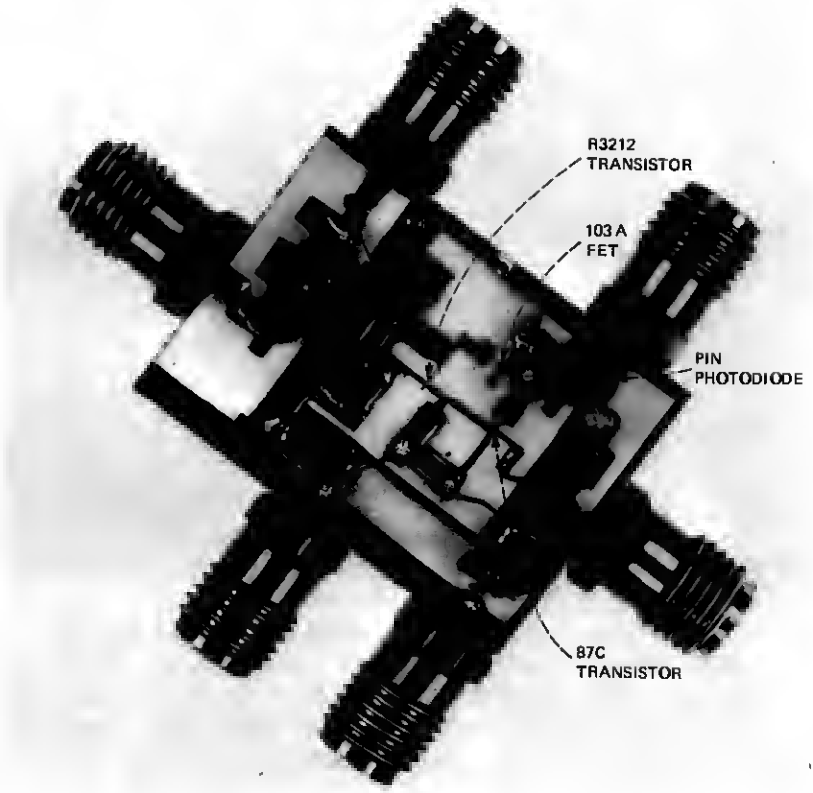

Fig. 10—Front-end module with coaxial test connections.

assumption that the LED and the fiber have infinite bandwidths. Actually, the LED bandwidth was 170 MHz, while the fibers used had bandwidths (3-dB optical) of 45 MHz in the 44.7-Mb/s experiment and 200 MHz in the 274-Mb/s experiment. As explained in Section III, these conditions lead to a modification of the J-values in eq. (2). If one uses eqs. (1), (5), and (6) to compute the penalty factors, the expected sensitivities become −48.2 dBm at 44.7 Mb/s and −36.8 dBm at 274 Mb/s.

The discrepancies from the measured data shown in Fig. 11 are 1.5 and 0.8 dB. We ascribe the difference at 44.7 Mb/s to induced gate noise and to the uncertainty in determining the actual amount of leakage current, which in our experiments fluctuated with humidity and near-term operating history. Tbe discrepancy at 274 Mb/s is probably a consequence of intersymbol interference which was neglected in our computation. However, the relatively good agreement

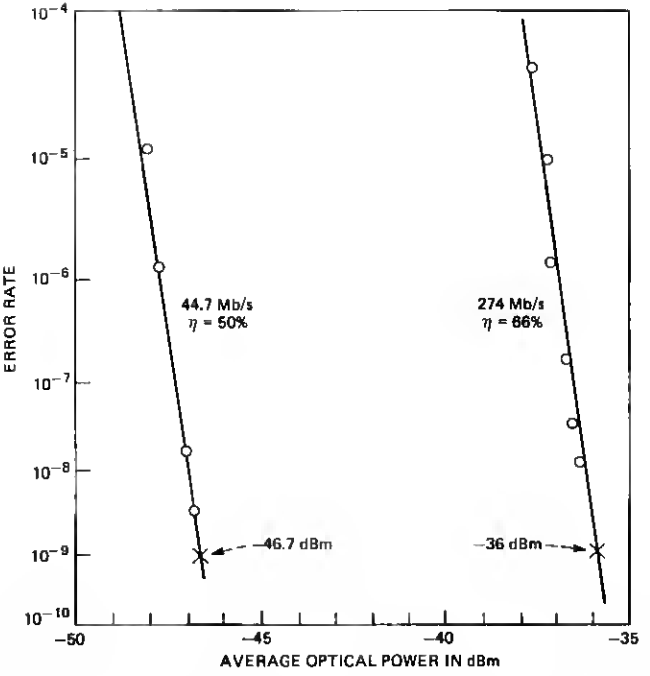

Fig. 11—Error rate vs average optical input power measured at 44.7 and 274 Mb/s.

gives us confidence that the equalization in the receiver can compensate for the known bandwidth limitations of the optical channel.

The remaining question of interest concerns the expected repeater spacing possible with LED-PIN systems operating at speeds above 40 Mb/s. Based on current research, the answer will naturally be conservative, but nevertheless it will provide an interesting benchmark. Allowing for component variations and elevated temperatures, we assume $g_m = 30$ mS, $C_T = 1.5$ pF, and $I_L = 200$ nA, and compute the average optical power $\bar{P}_r$ from eqs. (2) and (3), taking into account the LED modulation characteristics and fiber dispersion due to chromatic and intermodal delays; e.g., we use the appropriate J-coefficients in accordance with the actual transfer conditions as stipulated by eqs.

Table III—Pre-amplifier characteristics

Bit Rate Mb/s	Open Loop Gain	Feedback Resistance kΩ	Bandwidth (MHz)
44.7	30	500	3
274	12	30	50

(1), (5), and (6). This computation converts bandwidth limitations into an equalization penalty at the receiver. Lacking more specific information on intersymbol interference, we allow for an equalization penalty in decibels equal to the ratio zB/Q, where Q is the bandwidth-distance product resulting from intermodal delays. (This assumption is based on limited experimental experience and deserves further study.) In addition to these receiver sensitivity penalties, tbere are fixed margin (power-loss) allocations at the transmitter and tbe receiver as listed in Table IV.

The average LED output into a typical fiber (50-μm core, 0.23 N.A.) is assumed to be −13 dBm between 0 and 50 MHz, and to decrease by 2 dB between 50 and 100 MHz and by 3 dB/octave thereafter. The LED bandwidth is chosen for maximum signal margin $\bar{P}_s/\bar{P}_r$. This ratio, reduced by penalties and allocations, determines the transmission distance possible with a cable baving a given over-all loss. Since $\bar{P}_s/\bar{P}_r$ is a function of z because of eqs. (5) and (6), we must seek an iterative solution to determine z.

Some representative results are shown in Fig. 12. Cable loss and the bandwidth-distance product associated with intermodal dispersion are the two parameters used. We make the conservative assumption that the bandwidth decreases linearly with length. The transmission distances achievable range from 24 km at 44.7 Mb/s to 8 km at 274 Mb/s for cable having a loss of 1 dB/km and a bandwidth-distance product in the 1000-MHz·km range. The good agreement with experimental results seems to justify the underlying design rules. The influence of induced gate noise and the determination of residual intersymbol interference need further study.

Three interesting conclusions can be drawn from the calculation that resulted in Fig. 12:

(*i*) Loss limits the achievable repeater spacing more critically than bandwidtb. For a given application, the bandwidth specification and the associated equalization penalty allocation are design variables to be determined ultimately by economic considerations.

(*ii*) The "loss-limited" repeater spacing of LED-PIN systems varies

Table IV—Fixed margin allocations

Transmitter:	
30°C temperature rise	1.5 dB
Output decrease to end of life	1.5 dB
Connectors	1 dB
Receiver	
Feedback resistance	1 dB
Connectors	1 dB
Margin	3 dB
Total	9 dB

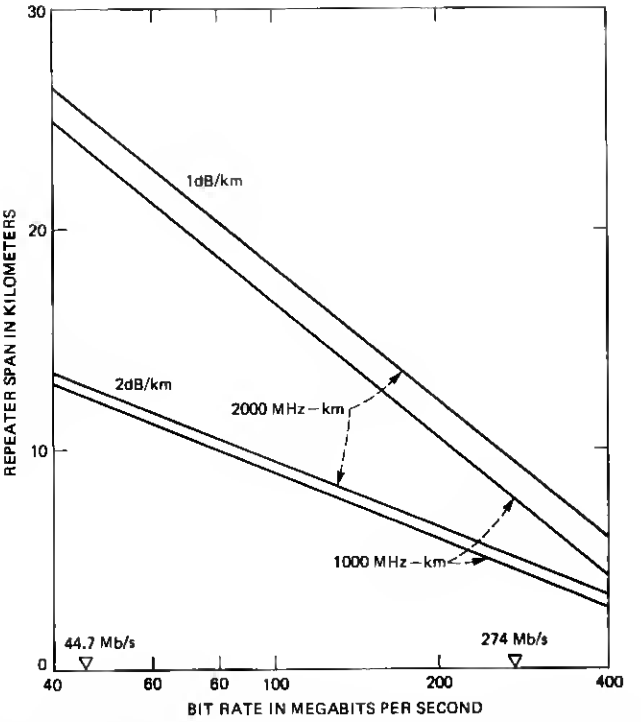

Fig. 12—Expected repeater distance versus bit rate for LED-PIN repeater at 1.3 μm; installed cable loss and bandwidth-distance product of fiber are the parameters.

approximately as the inverse of the bit rate in the range between 100 and 300 Mb/s. Therefore, since this implies a constant bit-rate-distance product, the bandwidth requirements are nearly the same for all these bit rates.

(*iii*) For a fiber bandwidth between 1000 and 2000 MHz·km and a spliced cable loss of ~1 dB/km and allowing a receiver equalization penalty of 2 to 4 dB, it is possible to build high-speed (≥100 Mb/s) LED-PIN systems with repeater spacings given in Fig. 12. Since the equalization penalty increases very rapidly with repeater spacing, an increase in source power (e.g., from the use of a laser) would permit larger margin allocations and penalties but would not lead to substantially longer repeater spacings in high-speed multimode systems.

VI. ACKNOWLEDGMENTS

We thank W. R. Northover, M. Saifi, and J. W. Shiever for the test fibers used, W. O. W. Schlosser and S. H. Wemple for their help with the GaAs FETs, W. Kruppa for providing the microwave transistors

and integrated circuits, and S. E. Miller for guidance and encouragement through all phases of this work.

REFERENCES

1. Tingye Li, "Optical Fiber Communication—The State of the Art," IEEE Trans. Commun., *COM-26* (1978), pp. 946–955.
2. D. Gloge, K. Ogawa, and L. G. Cohen, "Baseband Characteristics of Long-Wavelength LED Systems," Electr. Lett., *16* (1980), pp. 366–367.
3. W. M. Muska, Tingye Li, T. P. Lee, and A. G. Dentai, "Material-Dispersion-Limited Operation of High-Bit-Rate Optical-Fiber Data Links Using LEDs," Electr. Lett., *13* (1977), pp. 605–607.
4. S. Yamakoshi, M. Abe, S. Komiya, and Y. Toyama, "Degradation of High Radiance InGaAsP/InP LEDs at 1.2–1.3 μm Wavelength," Tech. Digest, Int. Elect. Dev. Meeting, Washington, D.C., December 3–5, 1979, pp. 122–124.
5. R. C. Goodfellow, A. C. Carter, I. Griffith, and R. R. Bradley, "GaInAsP/InP Fast High-Radiance, 1.05–1.3 μm Wavelength LEDs with Efficient Lens Coupling to Small Numerical Aperture Silica Optical Fibers," IEEE Trans. Elect. Dev., *Ed-26* (1979), pp. 1215–1220.
6. T. P. Lee and A. G. Dentai, "Power and Modulation Bandwidth of GaAs-AlGaAs High-Radiance LEDs for Optical Communication Systems," IEEE J. Quantum Electr., *QE-14* (1978), pp. 150–159.
7. H. Grothe, W. Proebster and W. Hart, "Mg-Doped InGaAsP/InP L.E.D.s for High-Bit-Rate Optical Communication Systems," Electr. Lett., *15*, (1979), pp. 702–703.
8. J. E. Goell, "Input Amplifiers for Optical PCM Receivers," B.S.T.J., *53* (1974), pp. 1771–1793.
9. D. R. Smith, R. C. Hooper, and I. Garrett, "Receivers for Optical Communications: A Comparison of Avalanche Photodiodes with PIN-FET Hybrids," Opt. Quant. Elect., *10* (1978), pp. 293–300.
10. D. R. Smith, R. C. Hooper, R. P. Wehh, and M. P. Saunders, "PIN Photodiode, Hyhrid Optical Receivers," Conf. Proc., Optical Communication Conference, Amsterdam, September 17–19, 1979, Paper 13.4.
11. K. Ogawa and E. L. Chinnock, "GaAsFET Transimpedance Front-end Design for a Wideband Optical Receiver," Electr. Lett., *15* (1979), pp. 660–653.
12. S. D. Personick, "Receiver Design for Digital Fiher Optic Communication Systems I and II," B.S.T.J., *52* (1973), pp. 843–886. See also R. G. Smith and S. D. Personick, "Receiver Design for Optical Fiher Communication Systems," Chapter IV in *Semiconductor Devices for Optical Communications*, H. Kressel, ed., New York: Springer Verlag, 1980.
13. W. Baechtold, "Noise Behavior of GaAs Field-Effect Transistors with Short Gate Lengths," IEEE Trans. Elect. Dev., *ED-19* (1972), pp. 674–680.
14. T. Takagi, "Spectral Half-Width of Spontaneous Emission of InGaAsP Lattice-Matched to InP," Jpn. J. Appl. Phys., *18* (1979), pp. 2017–2018.
15. A. G. Dentai, T. P. Lee, C. A. Burrus, "Small-Area High Radiance c.w. InGaAsP LEDs Emitting at 1.2 to 1.3 μm," Electr. Lett., *13* (1977), pp. 484–485.
16. T. P. Lee, C. A. Burrus, A. G. Dentai, and K. Ogawa, "Small Area InGaAs/InP PIN Photodiodes: Fabrication, Characteristics and Performance of Devices in 274 Mb/s and 45 Mb/s Lightwave Receivers at 1.3 μm Wavelength," Electr. Lett., *16* (1980), pp. 155–156.
17. R. F. Leheny, R. E. Nahory, and M. A. Pollack, "$In_{0.53}Ga_{0.47}$ As PIN Photodiodes for Long-Wavelength Fiber Optic Systems," Electr. Lett., *15* (1979), pp. 713–715.
18. F. D. Waldhauer, "A 2-Level, 274 Mb/s Regenerative Repeater for T4M," Conference Record, International Conference on Communications, June 16–18, 1975, San Francisco; pp. 48-13–48-17.
19. T. L. Maione, D. D. Sell, and D. H. Wolaver, "Practical 45 Mb/s Regenerator for Lightwave Transmission," B.S.T.J., *57* (1978), pp. 1837–1856.
20. S. H. Wemple, private communication.